RESEARCH/REVIEW ARTICLE

Palaeoenvironment of Eocene prodelta in Spitsbergen recorded by the trace fossil *Phycosiphon incertum*

Francisco Javier Rodríguez-Tovar,[1] Jenö Nagy[2] & Matías Reolid[3]

[1] Department of Stratigraphy and Palaeontology, University of Granada, Campus Fuentenueva sn, ES-18071 Granada, Spain
[2] Department of Geosciences, University of Oslo, PB 1047 Blindern NO-0316 Oslo, Norway
[3] Department of Geology, University of Jaén, Campus Las Lagunillas sn, ES-23071 Jaén, Spain

Keywords
Trace fossils; *Phycosiphon*; Eocene; prodelta; turbiditic sediments; Spitsbergen.

Correspondence
Francisco Javier Rodríguez-Tovar, Department of Stratigraphy and Palaeontology, University of Granada, Campus Fuentenueva sn, ES-18071 Granada, Spain. E-mail: fjrtovar@ugr.es

Abstract

Ichnological, sedimentological and geochemical analyses were conducted on the Eocene Frysjaodden Formation in order to interpret palaeoenvironment prodelta sediments in the Central Basin of Spitsbergen. *Phycosiphon incertum* is the exclusive ichnotaxon showing differences in size, distribution, abundance and density, and relation to laminated/bioturbated intervals. Large *P. incertum* mainly occur dispersed, isolated and randomly distributed throughout the weakly laminated/non-laminated intervals. Small *P. incertum* occur occasionally in patches of several burrows within laminated intervals or as densely packed burrows in thin horizons in laminated intervals or constituting fully bioturbated intervals that are several centimetres thick. Ichnological changes are mainly controlled by oxygenation, although the availability of benthic food cannot be discarded. Changes in oxygenation and rate of sedimentation can be correlated with the registered variations in the Bouma sequence of the distal turbiditic beds within prodeltal shelf sediments.

The upper part of the Palaeogene in the Central Basin of Spitsbergen (Svalbard region) comprises a progradation of an extensive coalesced delta system (Fig. 1). The basal part, the Frysjaodden Formation, is essentially a prodelta succession which is overlapped by the Battfjellet Formation, representing a prograding delta front locally with coast barrier bars. Above the Battfjellet Formation, the Aspelintoppen Formation is dominated by a coastal plain to delta plain system (Nagy 2005). In this general setting, a detailed characterization of the factors conditioning the environmental context is necessary.

Ichnological analysis can be used to interpret sedimentary environments, including ecological and depositional conditions (Rodríguez-Tovar & Uchman 2004a, b, 2006, 2010; Rodríguez-Tovar, Uchman & Martín-Algarra 2009; Rodríguez-Tovar, Uchman, Martín-Algarra et al. 2009; Rodríguez-Tovar, Uchman, Alegret et al. 2011; Rodríguez-Tovar, Uchman, Orue-Etxebarria et al. 2011; Knaust & Bromley 2012; Monaco et al. 2012; Rodríguez-Tovar et al. 2013). In deep-marine siliciclastic systems, which may include slopes or deep-sea fans, physico-chemical factors such as current energy, sedimentation rate, slope instability, substrate character, oxygen and food availability influence ichnological features such as the distribution, diversity, size and abundance of trace fossils. Therefore, ichnological analysis can be used to assess these parameters (Rodríguez-Tovar et al. 2010; Hubbard et al. 2012; Uchman & Wetzel 2012; Wetzel & Uchman 2012).

Another valuable approach to decipher environmental factors, including palaeoredox conditions and palaeoproductivity, is the use of geochemical proxies. Redox conditions in the water column and within the seafloor can be interpreted using redox-sensitive trace elements like Co, Ni and Mo, while the most extensively used proxies for palaeoproductivity reconstructions are Ba/Al, Sr/Al, Ca/Al and P/Ti ratios (see Reolid et al. 2012 and references therein).

The integration of both ichnological and geochemical data, together with sedimentological information, is a very informative strategy to elucidate interpretation of ecological and depositional conditions, which is applied in this paper to a prodelta succession of the Frysjaodden Formation in the Central Basin of Spitsbergen. The investigation is focused on trace fossil characterization, together with

Citation: *Polar Research* 2014, *33*, 23786, http://dx.doi.org/10.3402/polar.v33.23786

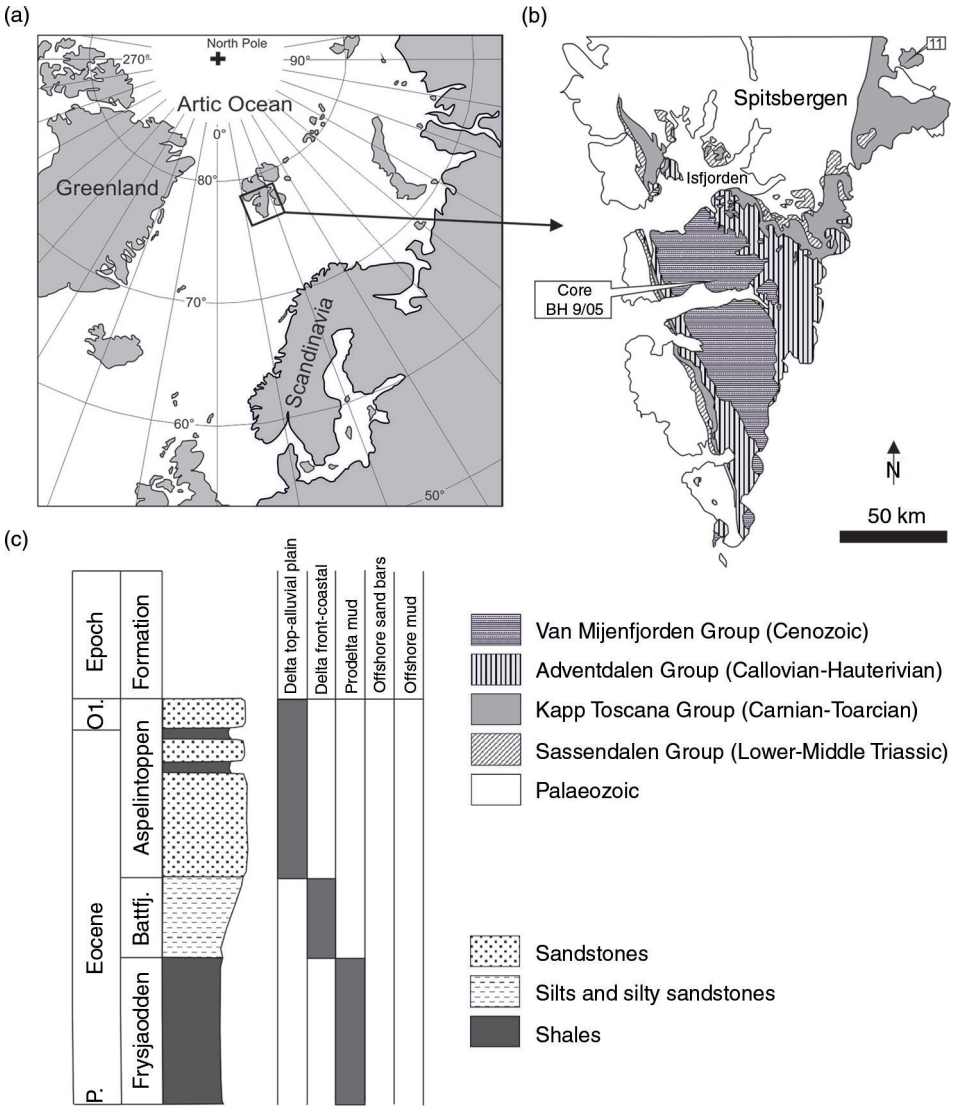

Fig. 1 Geological setting of the core samples from the borehole of the Store Norske Spitsbergen Grubekompani BH9/05. (a) General location of Spitsbergen. (b) Geological map of the south of Spitsbergen with drill site of core BH9/05. (c) Simplified succession of the Eocene of Spitsbergen with Frysjaodden Formation (Fm.), Battfjellet Formation and Aspelintoppen Formation and the interpreted palaeoenvironments (after Nagy et al. 2013).

geochemical analyses (palaeoproductivity and redox proxies) and the analysis of sedimentary features, in order to interpret ecological and depositional conditions. Special attention is placed on distal turbiditic sequences, which are more difficult to interpret than proximal ones since some of the diagnostic features (grain size, sedimentary structures, mineralogical components) do not vary significantly.

Geological setting and stratigraphy

The Palaeogene of Spitsbergen's Central Basin (Fig. 1) is a succession 2300 in thickness of mainly siliciclastic mudstones and sandstones deposited in fluvial, deltaic to delta-influenced marine shelf environments. They crop out mostly south of Isfjorden (Fig. 1). Their lithostratigraphy and depositional conditions have been discussed by, for example, Harland (1997), Dallmann et al. (1999) and Nagy (2005).

The Eocene deposits exhibit a coarsening-upward trend ranging from shales to sandstones, evidencing a transgression at the beginning of the Eocene and a subsequent regression. Three formations make up the Eocene succession: Frysjaodden, Battfjellet and Aspelintoppen (Fig. 1). They form the so-called Gilsonryggen Sequence, which commences with shoreline deposits, culminates in prodelta shelf mudstones, continues in delta front sandstones and terminates in the delta plain to alluvial

Citation: *Polar Research* 2014, *33*, 23786, http://dx.doi.org/10.3402/polar.v33.23786

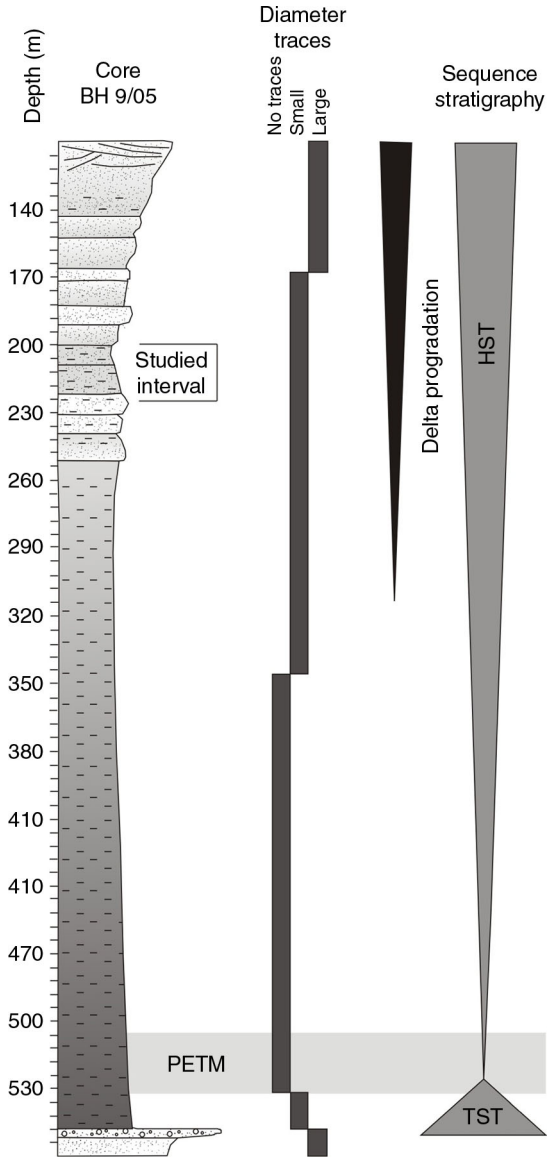

Fig. 2 Stratigraphic section inferred from core BH9/05. A general trend of the trace fossil diameters and system tracts is represented, together with the location of the interval analysed in this study (modified from Nagy et al. 2013). The following terms are abbreviated: highstand system tract (HST); transgressive system tract (TST); Palaeocene–Eocene Thermal Maximum (EPTM).

plain sandstones and mudstones of the Aspelintoppen Formation.

The studied borehole is located on the eastern flank of the Palaeogene Central Basin of Spitsbergen, south of Nordenskiöld Land, at Reindalen (ca. 77°50′N, 16°30′E; Fig. 1). The core, about 552 m long, includes the Gilsonryggen Member of the Frysjaodden Formation (from 552 to 112 m; Fig. 2), consisting of prodeltal shelf sediments with distal turbidites. Four parts can be differentiated in the Gilsonryggen Member (Figs. 1, 2).

Transitional beds occur at 552–533 m. A conglomerate bed at 552 m marks the lower boundary of the Gilsonryggen Member (Frysjaodden Formation). The basal 3 m consists of siltstone and fine-grained sandstone beds alternating with dark shales. This interval shows a fining-upward trend.

Lower shales occur at 533–344 m and consist of dark grey non-bioturbated shales commonly with fine lamination. Thin layers of bentonites occur at 517 and 511 m. From 500 m upwards, chert pebbles appear occasionally and are interpreted as dropstones transported on the thalli of floating seaweed (Nagy et al. 2013), but other interpretations as being ice-rafted deposits have been also proposed (Dalland 1977; Spielhagen & Tripati 2009). Siderite-cemented beds up to 1 cm thick appear at 500 m, increasing in frequency and thickness upwards. Decimetre-thick silty beds are typical of the upper part of the interval.

Middle shales occur at 344–166 m and consist of shales and subordinate siltstones and sandstones, principally concentrated in the upper part. From 242 m, a very weak upward-coarsening is observed, as seen in the increasing number and thickness of silt layers that usually contain dense but small trace fossils (see below). The upper part of this interval is characterized by large-scale upward-coarsening and upward-fining parasequences from silt to fine sand. Load structures are frequent, locally in combination with convolute lamination, suggesting high sedimentation rates (Dypvik et al. 2011). Ripple lamination is common and hummocky cross-stratification has been locally observed.

Uppermost sandy beds occur at 166–112 m and comprise sandstones and shales disposed in upward-coarsening sequences. Hummocky cross-bedding, wave-generated ripple lamination and load structures are common. Large trace fossils are abundant, principally in the mixed sand/shale interface. The top of the interval represents the boundary to the sandstones of the overlying Battfjellet Formation, with upward-coarsening lithology leading to cross-bedded sandstones in the topmost part. This influx of coarse-grained material reflects the progradation of the Battfjellet–Aspelintoppen delta system (Dypvik et al. 2011).

Turbiditic sequences are well represented in the middle shales. Hence, the selected study core, corresponding from 226.74 to 202.30 m, pertains to this facies.

Materials and methods

This research is based on core samples from borehole BH9/05 of the mining company Store Norske Spitsbergen Grubekompani.

Ichnological analysis focused on trace fossil characterization and ichnofabric analysis, with special attention to relative abundance, degree of bioturbation, distribution of burrows and relationships with lithology and sedimentary structures. Detailed observations of trace fossils were made on half-cut sections of selected intervals of the core. High-resolution images were obtained and several digital image techniques were applied to enhance trace fossil visibility (Dorador et al. 2014a, b, in press; Rodríguez-Tovar & Dorador 2014). Locally, the rock surface was wetted with water and/or light-weight oil—a "modified Bushinsky oil technique" (Bromley 1981).

Whole-rock analyses of major elements were carried out on 25 sampling levels using X-ray fluorescence in a PW 1040/10 spectrometer (Philips, Eindhoven, The Netherlands). The content of trace elements was determined using a Sciex-Elan 5000 inductively coupled plasma-mass spectrometer (Perkin Elmer, Waltham, MA, USA) at the Centro de Instrumentación Científica at the University of Granada. The instrumental error was $\pm 2\%$ and $\pm 5\%$ for elemental concentrations of 50 and 5 ppm, respectively.

Analysis of redox conditions in the seafloor is approached by means of redox-sensitive trace elements (such as Co, Cu, Mo and Ni) which tend to be less soluble under reducing conditions and become enriched under oxygen-depleted conditions (Wignall & Myers 1988; Calvert & Pedersen 1993; Jones & Manning 1994; Powell et al. 2003; Gallego-Torres et al. 2007; Gallego-Torres et al. 2010; Reolid et al. 2012). To compare trace element proportions in samples, it is usual to normalize element concentrations to aluminium content (Calvert & Pedersen 1993) to minimize lithological effects, assuming that Al content in sediments is contributed by aluminosilicates (e.g., Calvert 1990). The authigenic values for Mo were calculated according to Zhou et al. (2012) as $Mo_{aut} = [Mo]_{sample} - [Mo]_{PAAS}/[A1]_{PAAS} * [A1]_{simple}$. In addition, geochemical proxies are applied to interpret palaeoproductivity, the most extensively used being Ba/Al, Sr/Al and P/Ti ratios (e.g., Turgeon & Brumsack 2006; Gallego-Torres et al. 2007; Robertson & Filippelli 2008; Sun et al. 2008; Reolid & Martínez-Ruiz 2012; Reolid et al. 2012). Uranium and organic matter in the sediment are related in some sedimentary contexts as uranium may form a complex with dissolved fulvic acid in hemipelagic sediments (Nagao & Nakashima 1992). In this sense, the U/Al ratio can serve as a proxy for palaeoproductivity (Reolid et al. 2012).

Thin section analysis of intervals with trace fossils and intervals with parallel lamination was done using scanning electron microscopy with back-scattered electron images to determine the presence and size of pyrite framboids. Analyses were carried out with a Carl Zeiss Merlin microscope (Standort Göttingen, Vertrieb, Germany) at the Centro de Instrumentación Científico-Técnica at the University of Jaén, Spain. Framboid size distributions have been successfully applied as anoxia and euxinia indicators in fossil marine sediments (Wignall et al. 2005; Shen et al. 2007; Bond & Wignall 2010; Liao et al. 2010).

Results

Ichnological data include ichnotaxa features, trace fossil distribution within the studied section, relationships with laminated intervals and variations within turbiditic sequences. Geochemical data indicate variable relationships with laminated and bioturbated intervals.

The record of *Phycosiphon incertum*

Ichnological analysis in the studied section reveals the exclusive presence of *Phycosiphon incertum*. Trace fossils are characterized by small size, more or less cylindrical cores, and in some cases flattened, U-shaped lobes, as well as "fish-hook" shapes and pairs of black spots. Dark tubes consisting of fine-grained material are surrounded by a lighter mantle. Spreite structures were not observed, but this could be an effect of cutting. According to size, two groups of traces can be distinguished: (a) the small ones have observed tubes of a maximum length of 2–3 mm, 0.4–0.5 mm width, and marginal tubes approximately 0.2 mm wide; (b) the large forms have tubes 5–10 mm long, 0.8–1 mm wide, and marginal tubes 0.4 mm wide (Fig. 3). Small forms are dominant in the studied sections. The presented features allow to assign all the discussed trace fossils to *P. incertum* Fischer-Ooster.

According to the emended diagnosis by Wetzel & Bromley (1994), *P. incertum* refers to an extensive, small-scale spreite trace fossil consisting of repeated narrow, U-shaped lobes enclosing millimetre- to centimetre-scale spreite, branching regularly or irregularly from an axial spreite of similar width. Lobes are protrusive and mainly parallel to bedding, but the plane enclosing their width may lie horizontally, obliquely or even vertically with respect to the bedding plane. This is the widely accepted ichnotaxonomy by synonymization of *Anconichnus horizontalis* with *P. incertum*, emending the original identification of *P. incertum* by including non-bedding-parallel specimens, and showing *Anconichnus* as a junior synonym of *Phycosiphon*. A clear description of *P. incertum* is presented in Bromley (1996: 264–266). The author refers to a complexly-lobed, small-scale spreite structure, surrounded by a thin mantle of pale sediment; the core consists of backfilled dark material, and the spreite is made of the same pale material as the mantle. When mantle

Citation: *Polar Research* 2014, *33*, 23786, http://dx.doi.org/10.3402/polar.v33.23786

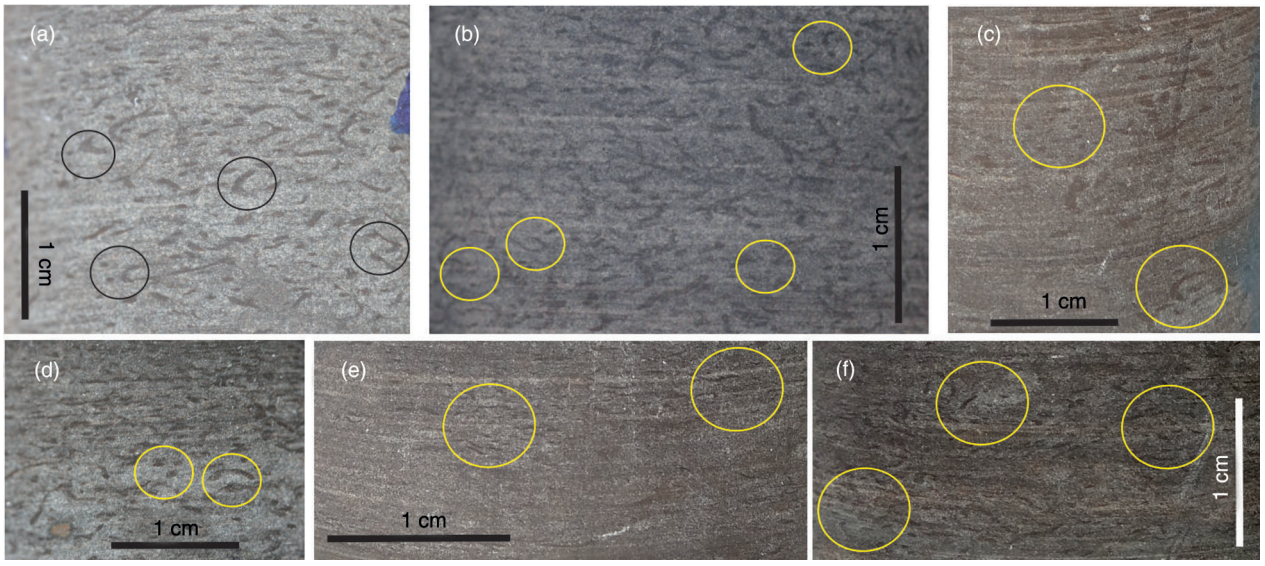

Fig. 3 Large and small *Phycosiphon incertum*. (a) – (c) Large *P. incertum*, showing more or less cylindrical cores, U-shaped lobes, fish-hook shapes and paired holes. Dark tubes are surrounded by a lighter mantle; in (a) and (b) this is interval 2; in (c) it is interval 1. (d) – (f) Small *P. incertum*, showing more or less cylindrical cores, usually flattened; in (d) this is interval 2; in (e) and (f) it is interval 1.

and spreite are difficult to detect, as in a pale matrix, the paired sections of fill where lobes are cut transversely, or "fish-hooks" where they are cut longitudinally, permit conclusive identification. Illustrative reconstructions of the multiple phases of foraging can be found, including three-dimensional models of "phycosiphoniform" burrows (i.e., figure 11.11 in Bromley 1996; Bednarz & McIlroy 2009). See Uchman (1995, 1998, 1999) for discussion of the *Phycosiphon* group, and ichnotaxonomy at the ichnospecies level.

Detailed analysis of *P. incertum* throughout the studied section reveals several patterns according to distribution, abundance and density, usually related to the differentiated size-groups: (a) sparsely and randomly distributed larger forms consisting of disperse, isolated *P. incertum* in a weakly to non-laminated intervals, with variable orientation in respect to the bedding plane, (b) sporadic records of small forms within a laminated interval, occurring as isolated specimens or as patches of several burrows with variable orientation, (c) densely packed small *P. incertum*, mainly parallel to the bedding plane, being located as horizons in laminated intervals and (d) densely distributed small forms (mainly horizontally) occupying a fully bioturbated interval several centimetres in thickness.

Laminated/bioturbated intervals in the studied section

Variations in *P. incertum* features within the laminated to bioturbated intervals include: (a) fully laminated intervals, consisting of millimetre-scale laminae with scarce or even absent *P. incertum*, (b) highly bioturbated intervals, either sparsely bioturbated with larger *P. incertum*, or intensely bioturbated intervals with small-sized forms and (c) bioturbated to laminated intervals, appearing as weakly laminated intervals with densely packed horizons or as patches of small *P. incertum*.

An idealized stratigraphic pattern of the differentiated cases is as follows: (a) at the base, a laminated interval with absent or only very scarce *P. incertum*; (b) above, a coarse-grained interval with cross-bedding lamination, showing a slightly undulated (erosional?) at the base and a gradual transition with a bioturbated interval at the top; and (c) finally, a gradual transition to a laminated interval with absent or very few *P. incertum*. This idealized pattern, however, may be present in a number of variations related to the presence of bioturbated horizons in the laminated/non-bioturbated interval (see below).

Trace fossil record and turbiditic sequences

The Gilsonryggen Member of the Frysjaodden Formation consists of prodelta sediments with distal turbidites. In the studied section, several cases were distinguished (Figs. 4, 5, 8).

Case A is present in the transition between successive turbiditic sequences: the transition shows a small erosional undulate-shape body composed of the massive—centimetre-thick—graded Ta interval of the Bouma sequence. It cuts into a laminated mud interpreted as the Te interval of the Bouma sequence below. This massive graded interval shows comparatively coarse grains, is lighter in

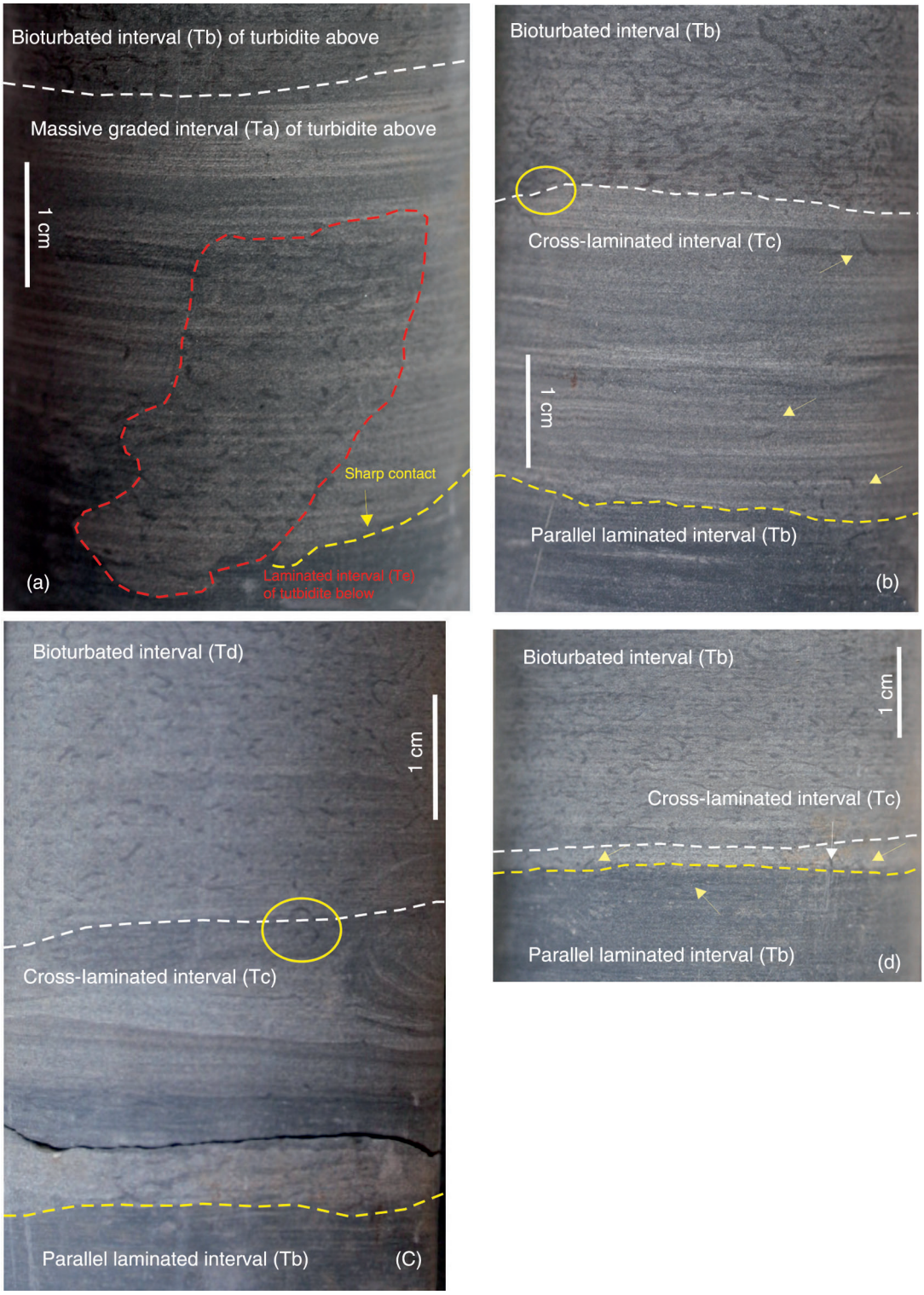

Fig. 4 (a) Transition between successive turbidic Bouma sequences, showing the thick massive (centimetre-thick) graded interval (Ta) of the Bouma sequence above into the upper laminated mud interval (Te) of the Bouma sequence below, as an erosional undulate-shaped body (Case A in Fig. 8). Note scarce, larger *Phycosiphon incertum* in Ta (interval 3; 226.72 cm). (b), (c) Centimetre-thick (Case B in Fig. 8) and (d) millimetre-thick (Case C in Fig. 8) cross-laminated interval (Tc) of the Bouma sequence registered above the lower laminated interval (Tb), with a slightly erosional undulated surface. Note scarce record of *P. incertum* (yellow arrows) at interval 2; 226.32 cm, 226.25 cm and 226.14 cm, for (b), (c) and (d), respectively).

Citation: *Polar Research* 2014, *33*, 23786, http://dx.doi.org/10.3402/polar.v33.23786

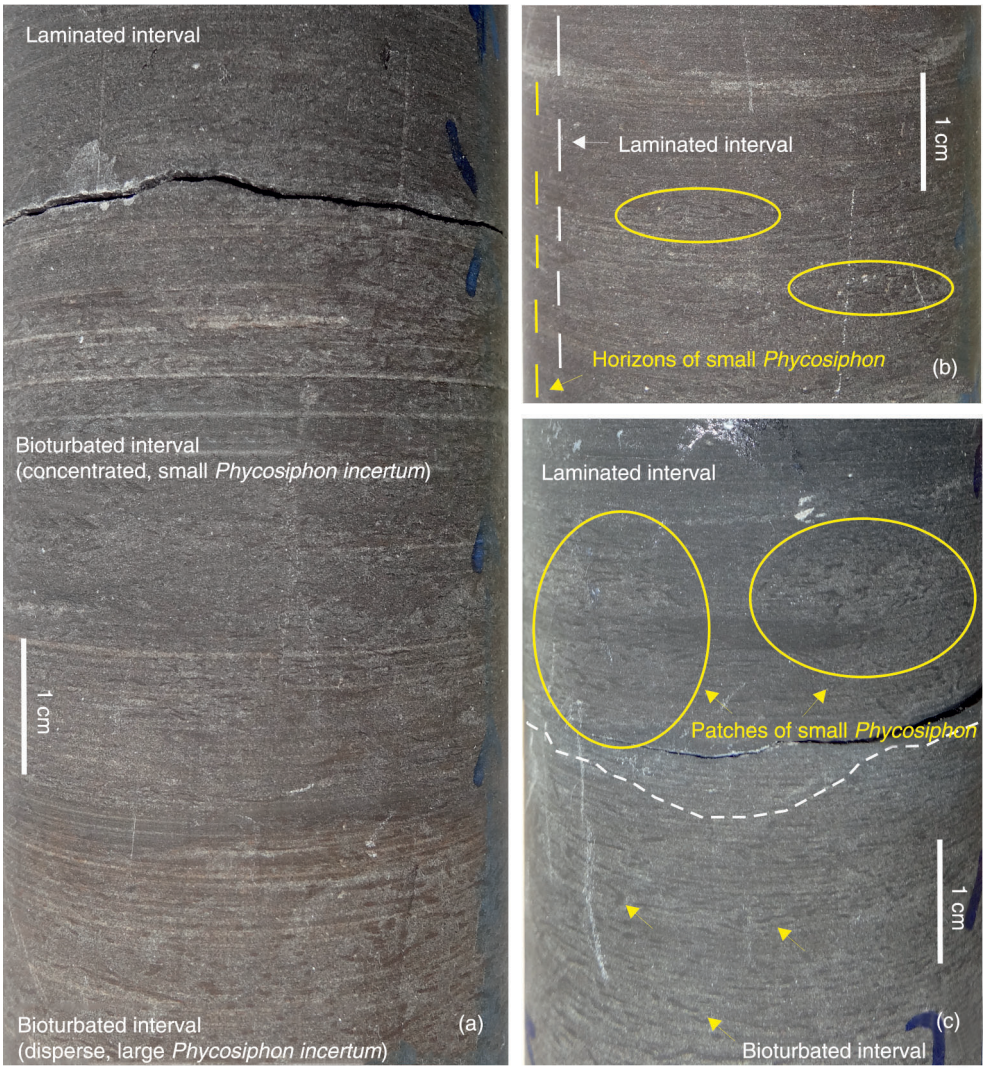

Fig. 5 Evolution in turbiditic Bouma sequence (Td–Te). (a) Case D in Fig. 8, showing gradual transition from a bioturbated interval with disperse, abundant, large *Phycosiphon incertum* to small, concentrated *Phycosiphon*, and then a laminated interval (interval 1; 222.52 cm). (b) Case E in Fig. 8, showing a laminated interval with horizons of small *Phycosiphon* and finally a laminated interval (interval 1; 222.66). (c) Case F in Fig. 8, showing the transition from a bioturbated interval with disperse, abundant, large *P. incertum* to a laminated interval with patches of small *Phycosiphon* and finely a laminated interval (interval 2; 226.26 cm).

colour, consisting of discrete, scarce, larger *P. incertum* (Fig. 4a). The laminated interval is characterized by the absence or scarce record of both, trace fossils and foraminifera.

Case B is observed in the middle part of a turbiditic sequence. A centimetre-thick cross-laminated interval Tc of the Bouma sequence is registered above the lower laminated interval Tb, with a slightly erosional undulated surface in between. The cross-laminated interval Tc is characterized by the absence/scarce record of *P. incertum* and foraminifera, as occurs in the former lower laminated interval (Fig. 4b, c).

Case C (middle part of a turbiditic sequence) is characterized by a millimetre-thick cross-laminated interval (Tc) above the lower laminated interval (Tb), with a slightly erosional undulating surface in between. This millimetre-thick cross-laminated interval also shows the absence or only scarce occurrence of *P. incertum*. This case is similar to case B, but associated to a thinner cross-laminated interval (Fig. 4d). In some cases, a cross-laminated interval is not observed; the bioturbated interval (Td) therefore overlies the laminated interval (Tb).

Case D refers to the middle–upper parts of the turbiditic sequence. A gradual transition from bioturbated to

laminated interval (Td–Te), showing progressively decreasing size and abundance of *P. incertum* and disappearance of the (scarce) foraminifera (Fig. 5a) is observed here.

Case E (middle–upper parts of the turbiditic sequence) shows a gradual transition from a bioturbated interval with disperse, abundant, large *P. incertum*, to a thick laminated interval showing alternating horizons with small *Phycosiphon* and thin laminated horizons (Td–Te) without bioturbational structures (Fig. 5b).

Case F (middle–upper parts of the turbiditic sequence) displays a gradual transition from a bioturbated interval with disperse, abundant, large *P. incertum*, to a thick laminated interval showing patches of small *Phycosiphon* and ending in a laminated horizon without bioturbational structures (Td–Te; Fig. 5c).

Geochemical proxies

Geochemical analyses of the studied section show a generalized pattern for all the studied proxies—the presence of long-term trends and the absence of short-term fluctuations, together with the presence of scattered, significant peaks of increasing geochemical values. The record of *Phycosiphon* is not directly related to increases in palaeoproductivity proxies, yet the peaks of redox proxies always occur in laminated horizons.

From the studied section, interval 1 (222.66–222.30 m; 34 cm thick) was selected to disclose the observed pattern (Fig. 6). All palaeoproductivity proxies (P/Ti, Ba/Al, Sr/Al and U/Al) show maximum values and a peak coinciding with horizons poorly-bioturbated by *Phycosiphon*. All redox proxies (Co/Al, Cu/Al, Ni/Al, Mo/Al and Mo_{aut}) show no variations along the studied interval, except for an important peak, with maximum values, just above the peak of the palaeoproductivity proxies, related to the well-laminated interval directly above the poorly-bioturbated horizons.

The analyses with back-scattered electron imagery reveal further differences between the well-laminated intervals and bioturbated intervals. The well-laminated intervals are richer in clay minerals, pyrite framboids and phytodetritus than the bioturbated intervals (Fig. 7). The size of the pyrite framboids is lower in well-laminated intervals (3.6–5.5 μm) than in bioturbated intervals (6.4–11.5 μm).

Interpretations and discussion

Ichnological and geochemical data: incidence of oxygenation and/or food availability

P. incertum traces are interpreted as having been produced by deposit feeders, usually opportunistic, at different tiers in mud and fine sand at variable depths up to 15 cm

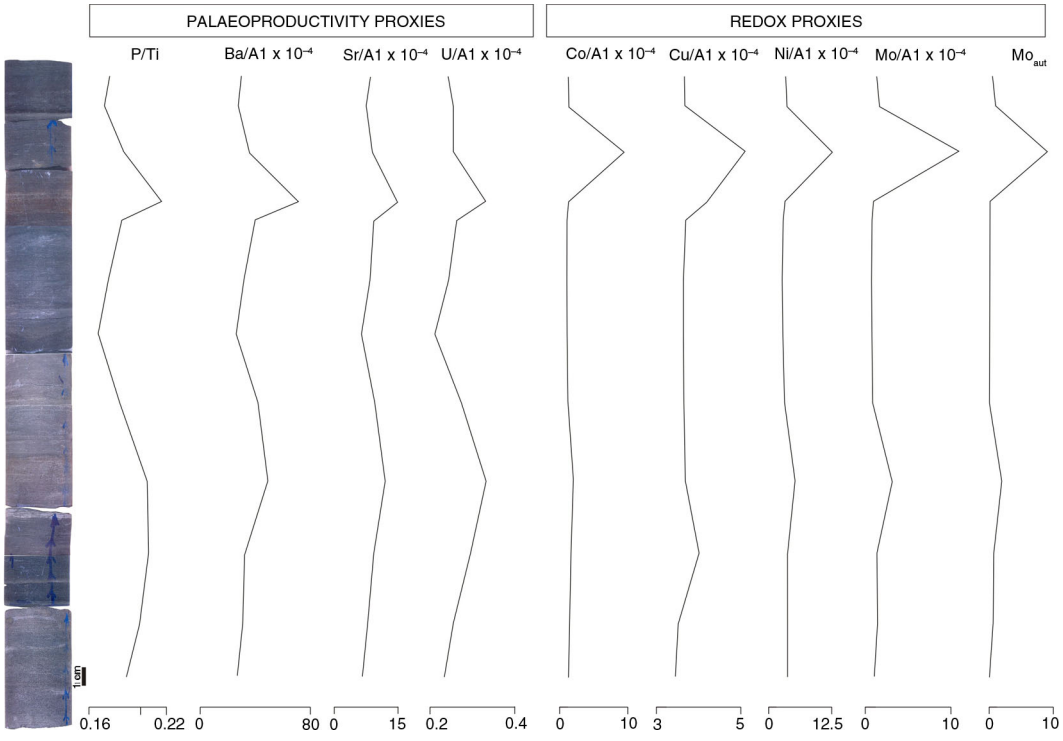

Fig. 6 Detailed stratigraphic distribution of the palaeoproductivity and redox proxies in interval 1 (222.66–222.30; 34 cm thick) of the studied section.

Citation: *Polar Research* 2014, *33*, 23786, http://dx.doi.org/10.3402/polar.v33.23786

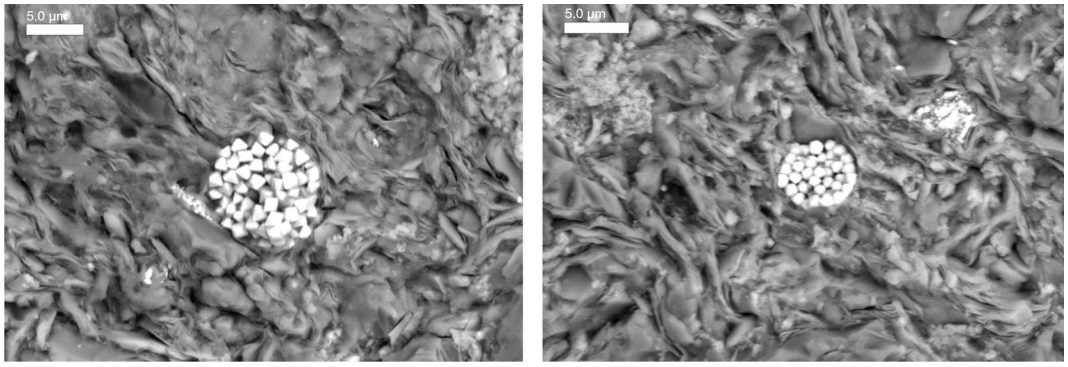

Fig. 7 Back-scattered electron image of pyrite framboids between clay minerals and quartz grains of the well-laminated intervals of the core. Scale bar 5 µm.

in sediments deposited in water depths below lower shoreface (Fu 1991; Goldring et al. 1991; Wetzel & Bromley 1994; Uchman 1995, 1999; Wetzel & Uchman 2001; Hovikoski et al. 2008; Wetzel 2010). *Phycosiphon* is considered a pascichnial/fodinichnial structure (Ekdale & Masson 1988; Bromley 1996); the absence of spreite was interpreted as reflecting a pascichnia (grazing) rather than a fodinichnia (mining) behaviour (Ekdale & Masson 1988). *Phycosiphon* traces have been observed in recent muddy mass-flow deposits in deep-marine settings, but the producer has not yet been recognized (Wetzel 2008). According to Bednarz & McIlroy (2009), producers of phycosiphoniform burrows were small, probably vermiform organisms.

Phycosiphon is frequently associated with food availability and oxygen conditions. The *Phycosiphon* producer reworked a relatively small volume of the sediment containing abundant nutritious material. Depth–size grading is typical of colonization; after initial colonization, the trace-maker grew in size and burrowed deeper into the sediment (Wetzel & Uchman 2001; Hovikoski et al. 2008). Orientation of *Phycosiphon* spreiten varies from inclined in homogeneous muds to horizontal in laminated deposits, probably reflecting the homogeneous distribution of food material (Wetzel & Uchman 2001; Wetzel 2010). *Phycosiphon* is common in poorly oxygenated sediments, but the absence of a connection to the seafloor indicates that immediate colonization took place in an oxygenated upper layer habitat (Ekdale & Masson 1988; Wetzel & Uchman 2001).

Integrated lithological and foraminiferal analyses of the core shed light on the general palaeoenvironmental conditions (Nagy et al. 2013). The upper part of the Gilsonryggen Member (Frysjaodden Formation) is related to the initial phases of delta progradation concomitant with the development of a highstand system tract. Salinity is a main restricting factor, though it decreases upward (Nagy et al. 2013), but short-term fluctuations may also be considered. The dominance of opportunistic organisms, such as that producing *P. incertum*, must be interpreted in the context of a stressed habitat resulting from salinity changes and fluctuations. However, the observed ichnological variations suggest the influence of additional environmental factors, including oxygenation and benthic food availability. The scarceness of foraminifera and the restricted occurrence of oxygen-tolerant forms

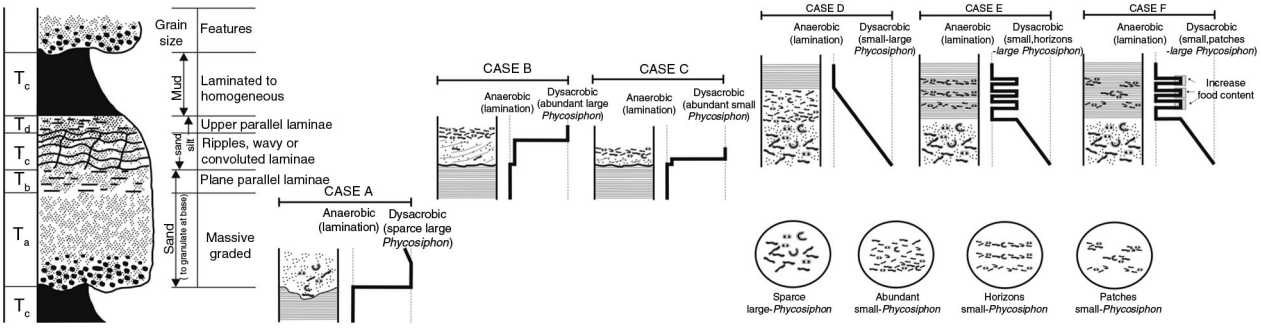

Fig. 8 Idealized Bouma sequence (Bouma 1962) and sketches of the cases (A–F) distinguished in the present study, with lithological and ichnological features, as well as oxygenation curves. See text for explanation.

(*Thurammina papillata*, *Psammosphaera fusca* and *Trochammina inornata* [Nagy et al. 2013]) would confirm the low oxygen availability.

The exclusiveness of *P. incertum*, the well-developed laminated intervals and the overall dark colour of the deposits all point to anoxic or highly dysoxic sediments. A minor increase in oxygen content to lower dysoxic conditions allowed for a localized colonization by the producer of *Phycosiphon*. The offset between the peak of palaeoproductivity proxies and the redox proxies may also be related to a consumption of oxygen resulting from increased productivity. Anoxic conditions are corroborated by the small size of pyrite framboids. Pyrite framboids only form at the redox boundary where oxygen-bearing and hydrogen sulphide-bearing waters are in contact (Wilkin et al. 1996; Reolid 2014). In oxygenated bottom water settings, pyrite framboid growth occurs in the upper sediment column, just below the sediment—water interface. However, in euxinic settings the redox boundary is within the water column. Framboids growing in the water column have a limited diameter range, as once they have grown to a certain size, they will sink out of the narrow redox interface zone and into oxygen-free bottom water and sediment where further growth is not possible (Wilkin et al. 1996; Dustira et al. 2013). The smallest mean diameters (3–5 μm) with a very limited size range are indicative of euxinic conditions (Bond & Wignall 2010). Framboids forming within the sediment under oxic bottom water conditions attain greater diameters on average (7.7 μm) as they reside and grow at the redox interface zone for a longer time (Wilkin et al. 1996). According to Wilkin et al. (1996) and Dustira et al. (2013), mean framboid size <7.7 μm indicates dysoxic conditions, between 5 and 7.7 μm corresponds to dysoxic—anoxic conditions and <5 μm indicates euxinic conditions. Taking into account these ranges of pyrite framboid size, the laminated intervals of study may have developed under euxinic conditions because the mean size observed was 3.6 μm. Since the mean size in the bioturbated intervals was 8.3 μm, framboids most likely developed in the sediment pore-water there.

Turbiditic sediments and ichnological record

Within deltaic systems, *Phycosiphon* has been observed mainly in sediments of the delta front, the transition zone between delta front and prodelta, and in the prodelta (i.e., Bann et al. 2008; Buatois et al. 2008; Carmona et al. 2009; Buatois et al. 2011; Weiguo et al. 2011; Buatois et al. 2012). Several papers addressed the immediate colonization of event beds by *Phycosiphon* trace-makers (Stow & Wetzel 1990; Goldring et al. 1991; Wetzel & Balson 1992; de Gibert & Martinell 1998). In muddy turbidites *Phycosiphon* producers are interpreted to be the first organisms colonizing the upper part of a turbidite bed, probably very rapidly, only a short time after deposition (Wetzel & Uchman 2001).

During delta progradation at the studied sections, turbidite deposition was extended, showing a succession of Bouma sequences. These Bouma sequences graded from massive sand deposits at the base to laminated silt and mud, with hemipelagic and pelagic material on top. Models of tiering, trace fossil distribution and ichnofabrics for turbidite/couplets have been proposed (Uchman 1999; Uchman & Wetzel 2011, 2012). Often, a sequential colonization of event layers can be found (Wetzel & Uchman 2001). Newly deposited turbiditic sediments contain relatively well-oxygenated pore water and a relatively high amount of benthic food, allowing initial colonization by small opportunistic deposit feeders, such as mining *Phycosiphon* producers. Later, when oxygen and food decrease at the level where mining as feeding strategy becomes inefficient, the sediment is colonized by stationary chemosymbionts, such as *Chondrites* producers. Finally, during the long period before deposition of a new turbidite, the slowly deposited background sediment is colonized by graphoglyptids in well-oxygenated settings (Uchman & Wetzel 2011, 2012). The studied case reveals clear differences with the model proposed by Uchman & Wetzel (2011, 2012), probably related to less favourable conditions, impeding a more diverse and better developed trace fossil assemblage.

When interpreting the turbiditic sediments in the studied section, the particular environmental conditions have to be taken into account, especially a long-term trend of decreasing salinity with short-term fluctuations, an oxygen content fluctuating between anaerobic and dysaerobic conditions, a short-term local input of benthic food and episodic sedimentation affecting all these factors. Variations in the ecological and sedimentological parameters would explain the variable record of the encountered Bouma sequences (Fig. 8) (e.g., Mulder 2011). Their variable development is interpreted according to the observed sedimentological and ichnological features associated with the transition between successive turbiditic sequences or within a single turbidite sequence (Fig. 8). We put forth six cases, as follows.

Case A: input of coarse sediment (Ta) was associated with an overall increase in oxygenation from the anaerobic laminated interval (Te) below to dysaerobic, conditions in Ta, probably related to a relatively high amount of food, allowing a disperse colonization of larger *Phycosiphon* trace-makers.

Citation: *Polar Research* 2014, *33*, 23786, http://dx.doi.org/10.3402/polar.v33.23786

Case B: deposition of the cross-laminated interval was not associated with an increase in oxygen content sufficient to allow a colonization by *Phycosiphon* trace-makers; anaerobic conditions during deposition of the upper part of the previous laminated interval (Tb) continued until the base of the next bioturbated interval (Td) above the cross-laminated interval was deposited.

Case C: this case, similar to case B, is characterized by a thin cross-laminated interval that could be related to rapid deposition of the cross-laminated interval or to minor erosion. Absent or only scarce *P. incertum* can be interpreted as reflecting persistent low-oxygen conditions (as in case B) or as evidence of a short time of deposition for the thin cross-laminated interval before deposition of the next interval (Td) which impeded colonization by *Phycosiphon* trace-makers.

Case D: this case could be associated with a gradual decrease in oxygen content from dysaerobic to finally nearly anaerobic conditions, documented by the colonization by large *Phycosiphon* trace-makers, then by small *Phycosiphon* and finally lacking bioturbation.

Case E: this case reflects a gradual decrease in oxygenation from dysaerobic conditions, allowing a colonization by large *Phycosiphon* trace-makers, to nearly anaerobic conditions generally preventing burrowing activities which are, registered only during short-time improvements in oxygenation.

Case F: in this case, the oxygen content decreased from dysaerobic conditions, allowing a colonization by large *Phycosiphon* trace-makers, to nearly anaerobic sediments strongly reducing the activity of *Phycosiphon* trace-makers. However, patches of *Phycosiphon* could be associated with short-time improvements in oxygenation together with localized patches of available benthic food, probably related to minor flows that brought oxygen and food from shallower zones.

Conclusions

Ichnological, sedimentological and geochemical analyses of sediments from the Eocene Frysjaodden Formation allow an interpretation of palaeonvironmental conditions during prodelta development in the Central Basin of Spitsbergen.

Ichnological analysis reveals the exclusiveness of *P. incertum* of different size showing variations in distribution, abundance and density: (a) large *P. incertum* are dispersed, isolated and randomly distributed throughout weakly/non-laminated intervals, with variable orientation with respect to the bedding; (b) small *P. incertum* occur sporadically in single, isolated, laminated intervals or in patches of variably oriented burrows; (c) densely packed small *P. incertum*, mainly horizontal to the bedding plane, are present in laminated horizons; and (d) densely distributed small *P. incertum* are found in fully bioturbated horizons which are several centimetres thick. These overall patterns reflect variable relationships of *P. incertum* and the distinguished laminated/bioturbated intervals. Variations in size, abundance and distribution of *P. incertum* can been related to oxygen contents fluctuating between anaerobic and dysaerobic conditions, short-time local inputs of benthic food and an episodic sedimentation affecting all these factors.

Several cases of distal turbiditic sequences conforming prodelta sediments could be distinguished according to the sedimentological and ichnological features found, mainly related to variable oxygenation and rates of sedimentation, determining variations in the Bouma sequence.

Acknowledgements

The paper benefited from comments and suggestions by two anonymous reviewers. Funding for this research was provided by Project CGL2012-33281 (Secretaría de Estado de Investigación, Desarrollo e Innovación, Spain), Project RYC-2009-04316 (Ramón y Cajal Programme) and Projects RNM-3715 and RNM-7408 and Research Group RNM-178 (Junta de Andalucía). The authors benefited from a bilateral agreement between the universities of Granada and Oslo, supported by the University of Granada.

References

Bann K.L., Tye S.C., MacEachern J.A., Fielding C.R. & Jones B.G. 2008. Ichnological and sedimentological signatures of mixed wave- and storm-dominated deltaic deposits: examples from the early Permian Sydney Basin, Australia. In G.J. Hampson et al. (eds.): *Recent advances in models of siliciclastic shallow-marine stratigraphy*. Pp. 293–332. Tulsa: Society of Economic Paleontologists and Mineralogists.

Bednarz M. & McIlroy D. 2009. Three-dimensional reconstruction of "phycosiphoniform" burrows: implications for identification of trace fossil in core. *Palaeontologia Electronica 12*, 12.3.13A.

Bond D.P.G. & Wignall P.B. 2010. Pyrite framboid study of marine Permian–Triassic boundary sections: a complex anoxic event and its relationship to contemporaneous mass extinction. *Geological Society of America Bulletin 122*, 1265–1279.

Bouma A.H. 1962. *Sedimentology of some Flysch deposits: a graphic approach to facies interpretation*. Amsterdam: Elsevier.

Bromley R.G. 1981. Enhancement of visibility of structures in marly chalk: modification of the Bushinsky oil technique. *Bulletin of the Geological Society of Denmark 29*, 111–118.

Bromley R.G. 1996. *Trace fossils: biology, taphonomy and applications*. London: Chapman and Hall.

Buatois L.A., Saccavino L.L. & Zavala C. 2011. Ichnologic signatures of hyperpycnal flow deposits in Cretaceous river-dominated deltas, Austral Basin, southern Argentina. In R.M. Slatt & C. Zavala (eds.): *Sediment transfer from shelf to deep water—revisiting the delivery system*. Pp. 153–170. Tulsa: American Association of Petroleum Geologists.

Buatois L.A., Santiago N., Herrera M., Plink-Björklund P., Steel R., Espin M. & Parra K. 2012. Sedimentological and ichnological signatures of changes in wave, river and tidal influence along a Neogene tropical deltaic shoreline. *Sedimentology 59*, 1568–1612.

Buatois L.A., Santiago N., Parra K. & Steel R. 2008. Animal–substrate interactions in an early Miocene wave dominated tropical delta: delineating environmental stresses and depositional dynamics (Tácata field, eastern Venezuela). *Journal of Sedimentary Research 78*, 458–479.

Calvert S.E. 1990. Geochemistry and origin of the Holocene sapropel in the Black Sea. In V. Ittekkot et al. (eds.): *Facets of modern biogeochemistry*. Pp. 326–352. Berlin: Springer.

Calvert S.E. & Pedersen T.F. 1993. Geochemistry of recent oxic and anoxic marine sediments: implications for the geological record. *Marine Geology 113*, 67–88.

Carmona N.B., Buatois L.A., Ponce J.J. & Mángano M.A. 2009. Ichnology and sedimentology of a tide-influenced delta, Lower Miocene Chenque Formation, Patagonia, Argentina: trace-fossil distribution and response to environmental stresses. *Paleogeography, Palaeoclimatology, Palaeoecology 273*, 75–86.

Dalland A. 1977. Erratic clasts in the lower Tertiary deposits of Svalbard—evidence of transport by winter ice. *Norsk Polarinstitutt Årbok 1976*, 151–165.

Dallmann W.K., Midbø P.S., Nøttvedt A. & Steel R.J. 1999. Tertiary lithostratigraphy. In W.K. Dallmann (ed.): *Lithostratigraphic lexicon of Svalbard*. Pp. 215–163. Tromsø: Norwegian Polar Institute.

de Gibert J.M. & Martinell J. 1998. Ichnofabric analysis of the Pliocene marine sediments of the Var Basin (Nice, SE France). *Geobios 31*, 271–281.

Dorador J., Rodríguez-Tovar F.J. & IODP Expedition 339 Scientists 2014a. Digital image treatment applied to ichnological analysis of marine core sediments. *Facies 60*, 39–44.

Dorador J., Rodríguez-Tovar F.J. & IODP Expedition 339 Scientists 2014b. Quantitative estimation of bioturbation based on digital image analysis. *Marine Geology 349*, 55–60.

Dorador J., Rodríguez-Tovar F.J. & IODP Expedition 339 Scientists. in press. A novel application of quantitative pixels analysis to trace fossil research in marine cores. *Palaios*.

Dustira A.M., Wignall P.B., Joachimski M., Blomeier D., Hartkopf-Fröder C. & Bond D.P.G. 2013. Gradual onset of anoxia across the Permian–Triassic boundary in Svalbard, Norway. *Palaeogeography, Palaeoclimatology, Palaeoecology 374*, 303–313.

Dypvik H., Riber L., Burca F., Rüther D., Jargvoll D., Nagy J. & Jochmann M. 2011. The Paleocene–Eocene Thermal Maximum in Svalbard—clay mineral and geochemical signals. *Palaeogeography, Palaeoclimatology, Palaeoecology 303*, 156–169.

Ekdale A.A. & Mason T.R. 1988. Characteristic trace-fossil associations in oxygen-poor sedimentary environments. *Geology 16*, 720–723.

Fu S. 1991. *Funktion, Verhalten und Einteilung fucoider und lophoctenoider Lebensspuren. (Function, behavior and classification of fucoides and lophoctenoides traces.) Courier Forschungsinstitut Senkenberg. Vol. 135*. Frankfurt: Senckenberg Natural Research Society.

Gallego-Torres D., Martínez-Ruiz F., Meyers P.A., Paytan A., Jiménez-Espejo F.J. & Ortega-Huertas M. 2010. Productivity patterns and N-fixation associated with Pliocene–Holocene sapropels: paleoceanographic and paleoecological significance. *Biogeosciences 8*, 415–431.

Gallego-Torres D., Martínez-Ruiz F., Paytan A., Jiménez-Espejo F.J. & Ortega-Huertas M. 2007. Pliocene–Holocene evolution of depositional conditions in the eastern Mediterranean: role of anoxia vs. productivity at 632 time of sapropel deposition. *Palaeogeography, Palaeoclimatology, Palaeoecology 246*, 424–439.

Goldring R., Pollard J.E. & Taylor A.M. 1991. *Anconichnus horizontalis*: a pervasive ichnofabric-forming trace fossil in post-Paleozoic offshore siliciclastic facies. *Palaios 6*, 250–263.

Harland W.B. 1997. *The geology of Svalbard*. London: Geological Society.

Hovikoski J., Lemiski R., Gingras M., Pemberton G. & MacEachern J.A. 2008. Ichnology and sedimentology of a mud-dominated deltaic coast: Upper Cretaceous Alderson Member (Lea Park Fm), western Canada. *Journal of Sedimentary Research 78*, 803–824.

Hubbard S.M., MacEachern J.A. & Bann K.L. 2012. Slopes. In D. Knaust & R. Bromley (eds.): *Trace fossils as indicators of sedimentary environments*. Pp. 607–642. Amsterdam: Elsevier.

Jones B.A. & Manning D.A.C. 1994. Comparison of geochemical indices used for the interpretation of paleoredox conditions in ancient mudstones. *Chemical Geology 111*, 111–129.

Knaust D. & Bromley R. (eds.) 2012. *Trace fossils as indicators of sedimentary environments*. Amsterdam: Elsevier.

Liao W., Wang Y.B., Kershaw S., Weng Z.T. & Yang H. 2010. Shallow-marine dysoxia across the Permian–Triassic boundary: evidence from pyrite framboids in the microbialite in South China. *Sedimentary Geology 232*, 77–83.

Monaco P., Rodríguez-Tovar F.J. & Uchman A. 2012. Ichnological analysis of lateral environmental heterogeneity within the Bonarelli level (uppermost Cenomanian) in the classical localities near Gubbio, Central Apennines, Italy. *Palaios 27*, 48–54.

Mulder T. 2011. Gravity processes and deposits on continental slope, rise and abyssal plains. In H. Hüneke & T. Mulder (eds.): *Deep-sea sediments*. Pp. 25–148. Amsterdam: Elsevier.

Nagao S. & Nakashima S. 1992. Possible complexation of Uranium with dissolved humic substances in pore water of marine-sediments. *Science of the Total Environment 118*, 439–447.

Citation: *Polar Research* 2014, *33*, 23786, http://dx.doi.org/10.3402/polar.v33.23786

Nagy J. 2005. Delta-influenced foraminiferal facies and sequence stratigraphy of Paleocene deposits in Spitsbergen. *Palaeogeography, Palaeoclimatology, Palaeoecology 222*, 161–179.

Nagy J., Jargvoll D., Dypvik H., Jochmann M. & Riber L. 2013. Environmental changes during the Paleocene–Eocene Thermal Maximum in Spitsbergen as reflected by benthic foraminifera. *Polar Research 32*, 19737, http://dx.doi.org/10.3402/polar.v32i0.19737.

Powell W.G., Johston P.A. & Collom C.J. 2003. Geochemical evidence for oxygenated bottom waters during deposition of fossiliferous strata of the Burgess Shale Formation. *Palaeogeography, Palaeoclimatology, Palaeoecology 201*, 249–268.

Reolid M. 2014. Pyritized radiolarians and siliceous sponges from oxygen restricted deposits (Lower Toarcian, Jurassic). *Facies 60*, 789–799.

Reolid M. & Martínez-Ruiz F. 2012. Comparison of benthic foraminifera and geochemical proxies in shelf deposits from the Upper Jurassic of the Prebetic (southern Spain). *Journal of Iberian Geology 38*, 449–465.

Reolid M., Rodríguez-Tovar F.J., Marok A. & Sebane A. 2012. The Toarcian Oceanic Anoxic Event in the western Saharan Atlas, Algeria (North African paleomargin): role of anoxia and productivity. *Geological Society of America Bulletin 124*, 1646–1664.

Robertson A.K. & Filippelli G.M. 2008. Paleoproductivity variations in the eastern equatorial Pacific over glacial timescales. *Abstract Eos, Transactions of the American Geophysical Union 89*(*53*), P33C–1576.

Rodríguez-Tovar F.J. & Dorador J. 2014. Ichnological analysis of Pleistocene sediments from the IODP Site U1385 "Shackleton Site" on the Iberian Margin: approaching palaeoenvironmental conditions. *Palaeogeography, Palaeoclimatology, Palaeoecology 409*, 24–32.

Rodríguez-Tovar F.J. & Uchman A. 2004a. Trace fossils after the K–T boundary event from the Agost section, SE Spain. *Geological Magazine 141*, 429–440.

Rodríguez-Tovar F.J. & Uchman A. 2004b. Ichnotaxonomic analysis of the Cretaceous/Palaeogene boundary interval in the Agost section, south-east Spain. *Cretaceous Research 25*, 635–647.

Rodríguez-Tovar F.J. & Uchman A. 2006. Ichnological analysis of the Cretaceous–Palaeogene boundary interval at the Caravaca section, SE Spain. *Palaeogeography, Palaeoclimatology, Palaeoecology 242*, 313–325.

Rodríguez-Tovar F.J. & Uchman A. 2010. Ichnofabric evidence for the lack of bottom anoxia during the lower Toarcian Oceanic Anoxic Event in the Fuente de la Vidriera section, Betic Cordillera, Spain. *Palaios 25*, 576–587.

Rodríguez-Tovar F.J., Uchman A., Alegret L. & Molina E. 2011. Impact of the Paleocene–Eocene Thermal Maximum on the macrobenthic community: ichnological record from the Zumaia section, northern Spain. *Marine Geology 282*, 178–187.

Rodríguez-Tovar F.J., Uchman A. & Martín-Algarra A. 2009. Oceanic anoxic event at the Cenomanian–Turonian boundary interval (OAE-2): ichnological approach from the Betic Cordillera, southern Spain. *Lethaia 42*, 407–417.

Rodríguez-Tovar F.J., Uchman A., Martín-Algarra A. & O'Dogherty L. 2009. Nutrient spatial variation during intrabasinal upwelling at the Cenomanian–Turonian oceanic anoxic event in the westernmost Tethys: an ichnological and facies approach. *Sedimentary Geology 215*, 83–93.

Rodríguez-Tovar F.J., Uchman A., Orue-Etxebarria X. & Apellaniz E.I. 2013. Palaeoenvironmental changes during the Danian–Selandian boundary interval: the ichnological record at the Sopelana section (Basque Basin, W Pyrenees). *Sedimentary Geology 284–285*, 106–116.

Rodríguez-Tovar F.J., Uchman A., Orue-Etxebarria X., Apellaniz E. & Baceta J.I. 2011. Ichnological analysis of the Bidart and Sopelana Cretaceous/Paleogene (K/Pg) sections (Basque Basin, W Pyrenees): refining eco-sedimentary environment. *Sedimentary Geology 234*, 42–55.

Rodríguez-Tovar F.J., Uchman A., Payros A., Orue-Etxebarria X., Apellaniz E.I. & Molina E. 2010. Sea-level dynamics and palaeoecological factors affecting trace fossil distribution in Eocene turbiditic deposits (Gorrondatxe section, N Spain). *Palaeogeography, Palaeoclimatology, Palaeoecology 285*, 50–65.

Shen W.J., Lin Y.T., Xu L., Li J.F., Wu Y.S. & Sung Y.G. 2007. Pyrite framboids in the Permian–Triassic boundary section at Meishan, China: evidence for dysoxic deposition. *Palaeogeography, Palaeoclimatology, Palaeoecology 253*, 323–331.

Stow D.A.V. & Wetzel A. 1990. Hemiturbidite: a new type of deep-water sediment. In J.R. Cochran et al. (eds.): *Proceedings of the Ocean Drilling Project. Scientific results. Vol. 116.* Pp. 25–34. College Station, TX: Ocean Drilling Program.

Spielhagen R.F. & Tripati A. 2009. Evidence from Svalbard for near-freezing temperatures and climate oscillations in the Artic during the Paleocene and Eocene. *Palaeogeography, Palaeoclimatology, Palaeoecology 278*, 48–56.

Sun Y.B., Wu F., Clemens S.C. & Oppo D.W. 2008. Processes controlling the geochemical composition of the South China Sea sediments during the last climatic cycle. *Chemical Geology 257*, 234–249.

Turgeon S. & Brumsack H.J. 2006. Anoxic vs. dysoxic events reflected in sediment geochemistry during the Cenomanian–Turonian Boundary Event (Cretaceous) in the Umbria-Marche basin of central Italy. *Chemical Geology 234*, 321–339.

Uchman A. 1995. Taxonomy and palaeoecology of flysch trace fossils: the Marnoso-arenacea Formation and associated facies (Miocene, Northern Apennines, Italy). *Beringeria 15*, 3–115.

Uchman A. 1998. Taxonomy and ethology of flysch trace fossils: revision of the Marian Ksiazkiewicz collection and studies of complementary material. *Annales Societatis Geologorum Poloniae 68*, 105–218.

Uchman A. 1999. Ichnology of the Rhenodanubian Flysch (Lower Cretaceous-Eocene) in Austria and Germany). *Beringeria 25*, 67–173.

Uchman A. & Wetzel A. 2011. Deep-sea ichnology: the relationships between depositional environment and en-

dobenthic organisms. In H. Hüneke & T. Mulder (eds.): *Deep-sea sediments*. Pp. 517–556. Amsterdam: Elsevier.

Uchman A. & Wetzel A. 2012. Deep-sea fan. In D. Knaust & R.G. Bromley (eds.): *Trace fossils as indicators of sedimentary environments*. Pp. 643–672. Amsterdam: Elsevier.

Weiguo L., Bhattacharya J.P. & Yingmin W. 2011. Delta asymmetry: concepts, characteristics, and depositional models. *Petroleum Science 8*, 278–289.

Wetzel A. 2008. Recent bioturbation in the deep South China Sea: a uniformitarian ichnologic approach. *Palaios 23*, 601–615.

Wetzel A. 2010. Deep-sea ichnology: observations in modern sediments to interpret fossil counterparts. *Acta Geologica Polonica 60*, 125–138.

Wetzel A. & Balson P. 1992. Sedimentology of fine-grained turbidites inferred from continuously recorded physical properties data. *Marine Geology 104*, 165–178.

Wetzel A. & Bromley R.G. 1994. *Phycosiphon incertum* revisited: *Anconichnus horizontalis* is its junior subjective synonym. *Journal of Paleontology 60*, 1396–1402.

Wetzel A. & Uchman A. 2001. Sequential colonization of muddy turbidites in the Eocene Beloveža Formation, Carpathians, Poland. *Paleogeography, Palaeoclimatology, Palaeoecology 168*, 171–186.

Wetzel A. & Uchman A. 2012. Hemipelagic and pelagic basin plains. In D. Knaust & R.G. Bromley (eds.): *Trace fossils as indicators of sedimentary environments*. Pp. 673–701. Amsterdam: Elsevier.

Wignall P.B. & Myers K.J. 1988. Interpreting the benthic oxygen levels in mudrocks: a new approach. *Geology 16*, 452–455.

Wignall P.B., Newton R. & Brookfield M.E. 2005. Pyrite framboid evidence for oxygen-poor deposition during the Permian–Triassic crisis in Kashmir. *Palaeogeography, Palaeoclimatology, Palaeoecology 216*, 183–188.

Wilkin R.T., Barnes H.L. & Brantley S.L. 1996. The size distribution of framboidal pyrite in modern sediments: an indicator of redox conditions. *Geochimica et Cosmochimica Acta 60*, 3897–3912.

Zhou L., Wignall P.B., Su J., Feng Q., Xie S., Zhao L. & Huang J. 2012. U/Mo ratios and d98/95Mo as local and global redox proxies during mass extinction events. *Chemical Geology 324–325*, 99–197.